Chinese Chemical Letters 37 (2026) 111158

Contents lists available at ScienceDirect

Chinese Chemical Letters

journal homepage: www.elsevier.com/locate/cclet

Hourglass-shaped organophosphomolybdate(V) as photoelectrochemical sensor for selective detection of trace levofloxacin

Meng-Si Guo, Chun-Xiao Yin, Zi-Yi Zhang, Yuan-Yuan Ma*, Jing Du*, Zhan-Gang Han*

Hebei Technology Innovation Center for Energy Conversion Materials and Devices, Hebei Engineering Research Center of Thin Film Solar Cell Materials and Devices, National Demonstration Center for Experimental Chemistry Education, College of Chemistry and Materials Science, Hebei Normal University, Shijiazhuang 050024, China

ARTICLE INFO

Article history:
Received 20 January 2025
Revised 18 March 2025
Accepted 27 March 2025
Available online 27 March 2025

Keywords:
Polyoxometalate
Hourglass-shaped organophosphomolybdate
Functionalization
Photoelectrochemical sensor
Levofloxacin detection

ABSTRACT

Phenylphosphonate functionalized fully-reduced hourglass-shaped organophosphomolybdate(V) hybrid $(H_2bib)\{Ni[Mo_6(PO_3C_6H_5)_4O_{15}H_6]_2\}\cdot 9H_2O$ (bib = 4,4′-bis(imidazolyl)bibpheny) was synthesized as a photoelectrochemical (PEC) sensor. Benefiting from the electron transfer interaction between organic phenyl groups and inorganic $\{P_4Mo_6\}$ skeleton, compound achieved a low detection limit of 4.61 nmol/L and high sensitivity of 264.02 μA L/μmol toward the PEC detection of levofloxacin in aqueous solution, together with excellent practicality in milk sample.

© 2026 Published by Elsevier B.V. on behalf of Chinese Chemical Society and Institute of Materia Medica, Chinese Academy of Medical Sciences.

Reduced polyoxometalates (POMs) have attracted increasing attention owing to their unique functional properties and desirable merits in a wide range of applications, including material science, environment and photo/electrochemical catalysis [1–3]. Among them, fully-reduced hourglass-shaped phosphomolybdate cluster, denoted as $\{M[P_4Mo^V{}_6O_{31}]_2\}^{n-}$ (*abbr.* as $M\{P_4Mo_6\}_2$), represents a distinctive anionic species featuring all Mo sites in the +5 oxidation state, which are assembled by linking two identical $[P_4Mo^V{}_6O_{31}]^{12-}$ subunits through a central bridging metal M atom [4]. Benefiting from the fully reduced oxidation state of Mo(V), $M\{P_4Mo_6\}_2$ clusters demonstrate outstanding redox properties, robust electron transfer capabilities and extensive spectral absorption range from the UV–visible to near-infrared regions, rendering them promising candidates for applications in energy, catalysis and photoelectrochemical (PEC) sensing [5–8].

Nowadays, the covalent functionalization of POM surface with organic ligands has been considered as an efficient strategy to impart novel functionalities [9–12]. Since Haushalter and Zubieta *et al.* reported the first ammonium salt of phenylphosphonate-functionalized $Na\{P_4Mo_6\}_2$ cluster in 1993, the field of organophosphonate-functionalized $M\{P_4Mo_6\}_2$ has progressed at a leisurely pace, which may be due to the complex synthetic requirements [13]. So far, there are only five examples of organophosphonate-functionalized $M\{P_4Mo_6\}_2$ (M = Na, K) clusters, and these works only focused on the synthesis condition regulation of $\{Na[Mo_6O_{12}(OH)_3(O_3PC_6H_5)_4]_2\}^{9-}$ cluster [14,15]. The influence and interaction mechanism of organophosphonate covalent functionalization on the properties of $M\{P_4Mo_6\}_2$ clusters have not yet been documented. Therefore, achieving the directed synthesis and functional expansion of organophosphonate-functionalized $M\{P_4Mo_6\}_2$ continues to be a significant research domain within POM chemistry, which contributes to the formation of complex molecular architectures and the emergence of new, unique functionalities.

Herein, a kind of phenylphosphonate-functionalized $Ni\{P_4Mo_6\}_2$-based hybrid, with formula of $(H_2bib)\{Ni[Mo_6(PO_3C_6H_5)_4O_{15}H_6]_2\}\cdot 9H_2O$ (**1**) (bib = 4,4′-bis(imidazolyl)bibpheny), was hydrothermally synthesized as a PEC sensor. Benefiting from the electron transfer interaction between organic phenyl groups and inorganic $\{P_4Mo_6\}$ skeleton, compound **1** displayed a broader spectral absorption and reversible redox property compared to the pure inorganic $Ni\{P_4Mo_6\}_2$ cluster, and showed excellently sensitive and selective PEC detection performance toward levofloxacin with a low detection limit of 4.61 nmol/L and a high sensitivity of 264.02 μA L/μmol in aqueous solution. At the same time, the sensor also showed good performance on levofloxacin in the real milk samples.

* Corresponding authors.
E-mail addresses: mayy334@hebtu.edu.cn (Y.-Y. Ma), duj622@hebtu.edu.cn (J. Du), hanzg116@hebtu.edu.cn (Z.-G. Han).

https://doi.org/10.1016/j.cclet.2025.111158
1001-8417/© 2026 Published by Elsevier B.V. on behalf of Chinese Chemical Society and Institute of Materia Medica, Chinese Academy of Medical Sciences.

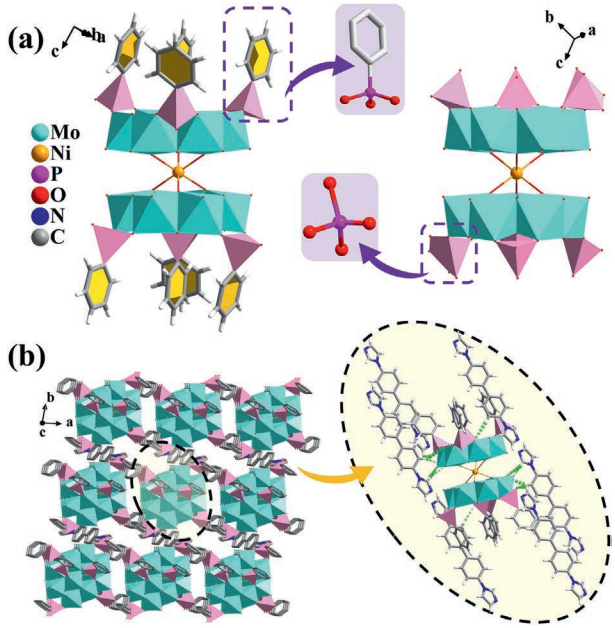


Fig. 1. (a) Structural comparison of phenylphosphonate-functionalized Ni{$(PhP)_4Mo_6$}$_2$ and pure inorganic Ni{P_4Mo_6}$_2$ cluster. (b) Supramolecular stacking structure of compound **1**, insert: C-H···O interactions among organic moieties in compound **1**.

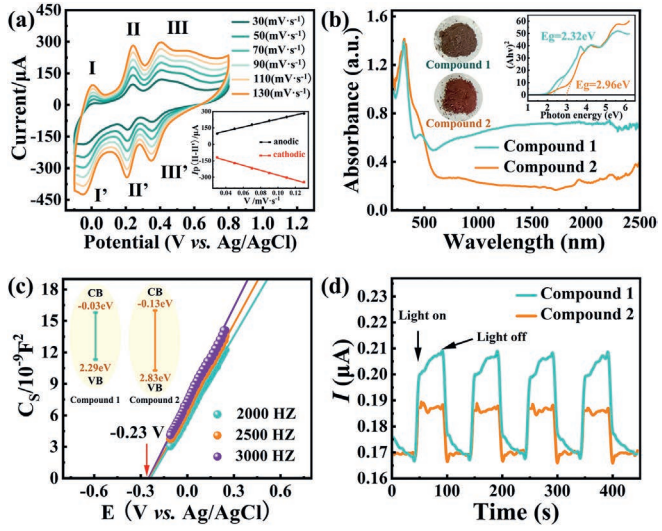


Fig. 2. (a) CV plots for compound **1** across various scanning rates. (b) UV–Vis-NIR diffuse reflectance spectra of compounds **1-2** (inserts: band gap energies). (c) Mott–Schottky plots for compound **1** and energy levels diagram of the CB and VB of compounds **1-2**. (d) Periodic (on/off) photocurrent behaviors of compounds **1-2**.

Single-crystal X-ray diffraction analysis showed that compound **1** presented a supramolecular structure composed of protonated $\{Ni[Mo^V_6(PO_3C_6H_5)_4O_{15}H_6]_2\}^{2-}$ cluster (denoted as Ni{$(PhP)_4Mo_6$}$_2$) and protonated $[H_2bib]^{2+}$ cation (Tables S1-S4 in Supporting information). As shown in Fig. 1a and Fig. S1 (Supporting information), Ni{$(PhP)_4Mo_6$}$_2$ cluster features an hourglass-shaped structure, which consists of two $[Mo_6O_{15}(O_3PC_6H_5)_4H_6]^{2-}$ (*abbr*. as {$(PhP)_4Mo_6$}) half-units bridged by one Ni^{2+} ion. The {$(PhP)_4Mo_6$} half-unit is composed of four {PhP} groups and six {MoO_6} octahedra. Among them, the {MoO_6} octahedra are interconnected *via* edge-shared to form a planar {Mo_6} six-membered ring structure. Three {PhP} groups are bonded to the edges of the {Mo_6} six-membered ring in a C_3-symmetric manner, and one {PhP} group is located at the center of the {Mo_6} six-membered ring. In compound **1**, the protonated $[H_2bib]^{2+}$ cations occupy the intervals among Ni{$(PhP)_4Mo_6$}$_2$ clusters, and there are significant C-H···O, C-H···π and anion···π interactions between them, further promoting the stability of 3D hybrid structure (Fig. 1b, Fig. S2 and Table S5 in Supporting information).

The composition and structure of compound **1** was characterized by FT-IR spectroscopy, XRD and TG analysis. The IR spectrum of compound **1** exhibits distinctive peaks at 558–1151 cm^{-1} (Fig. S3 in Supporting information), which can be ascribed to the stretching vibrations of P-O, Mo-O and Mo-O-Mo bonds within the cluster. The strong characteristic peaks in the range of 1490-1602 cm^{-1} correspond to the C=C and C=N stretching vibrations of the N-containing organic components. A different peak at 1440 cm^{-1}, which can be ascribed to the stretching vibrations of P-Ph bonds within the compound **1**. The XRD pattern of the synthesized compound **1** aligned well with the theoretical simulation result, signifying its good phase and high crystallinity (Fig. S4 in Supporting information). TG analysis revealed that the structure of compound **1** could be maintained up to 270 °C (Fig. S5 in Supporting information), demonstrating its robust thermal stability.

To explore the influence of organophosphonate covalent functionalization on the properties of Ni{P_4Mo_6}$_2$ cluster, another compound with formula of $(H_2bib)_2[H_2PO_4][Ni(P_4Mo_6O_{31}H_{9.5})_2]\cdot 17H_2O$ (**2**) was synthesized, which exhibited similar structural arrangement as compound **1** except that the phenylphosphonate groups were replaced by inorganic phosphates (Fig. 1a, Fig. S6 and Tables S6-S8 in Supporting information). Fig. 2a and Fig. S7 (Supporting information) show the cyclic voltammetry (CV) curves of compounds **1-2**. It can be found that there are three pairs of reversible redox peaks in the voltage window from −0.1 V to 0.8 V, which were associated with the two-, four-, and six-electron transfer processes by Mo atoms of Ni{$(PhP)_4Mo_6$}$_2$/Ni{P_4Mo_6}$_2$ clusters [16], revealing the excellent redox activities of compounds **1-2** (Table S9 in Supporting information). Moreover, as the scan rate rises, the peak currents gradually increase but the peak positions basically keep unchanged. Represented by the second pair of redox peaks, a linear correlation exists between the square root of the scanning speeds and the peak currents, signifying their excellent electrochemical stability and the diffusion predominantly dictates the redox activity on the catalyst surface. Compared with compound **2**, compound **1** not only exhibited the more ideal and reversible electrochemical process, but also presented the more sensitive current response at the same sweep speed, indicating the higher electrochemical activity of compound **1**.

Furthermore, the optical behaviors of compounds **1-2** were tested using solid-state UV–vis-NIR diffuse reflectance spectroscopy and the Mott-Schottky methods. As depicted in Fig. 2b, compounds **1-2** display continuous absorption characteristics within a wide wavelength range from 200 nm to 2500 nm. Two compounds exhibit similar strong light absorption bands in the UV–vis region (200–500 nm), which can be attributed to the charge transfer of O→Mo^V in the fully-reduced Ni{$(PhP)_4Mo_6$}$_2$ and Ni{P_4Mo_6}$_2$ clusters. However, in the visible-near infrared region (500–2500 nm), compound **1** showed stronger light absorption ability than compound **2**. This result implies that the phenylphosphonate covalent functionalization can enhance the light absorption of Ni{P_4Mo_6}$_2$ cluster across the full spectrum. Based on the formula $(\alpha h\nu)^2 = A(h\nu - E_g)^n$ [17], the band gaps (E_g) of **1-2** are calculated to be 2.32 V and 2.96 V, respectively (Fig. 2c insert). The narrower bandgap of compound **1** may be due to the interaction between the phenyl groups and the reduced phosphomolybdate clusters, which regulated the arrangement of energy levels and enhanced the light absorption capacity. The Mott–Schottky plots in

Fig. 2c and Fig. S8 (Supporting information) further revealed that the flat band potentials of compounds **1-2** are −0.23 V and −0.33 V (*vs.* Ag/AgCl), from which the conduct bands (CB) are obtained to be −0.03 V *vs.* NHE for **1** and −0.13 V *vs.* NHE for **2**, respectively. By combining the data from the UV–vis-NIR spectroscopy, the valence band (VB) positions of compounds **1-2** are determined as 2.29 V *vs.* NHE for **1** and 2.83 V for **2**. The VB potentials of compounds **1-2** are more positive than the oxidation potentials of H_2O/O_2 (+1.23 V), $H_2O/O_2^{\cdot-}$ (+1.44 V) and $H_2O/{\cdot}OH$ (+2.27 V) [18,19], indicating that the photooxidation of LVF by these compounds are thermodynamically possible. Furthermore, to evaluate the photoinduced charge separation efficiency, the transient photocurrent response experiments were carried out under visible light irradiation. Compound **1** produces a transient photocurrent of 0.045 μA, which is 2.25 times higher than that of compound **2** (0.02 μA) (Fig. 2d). In view of the fact that compounds **1-2** possess similar supramolecular arrangements except the phenylphosphonate covalent functionalization on $Ni\{P_4Mo_6\}_2$ cluster. This result further reveals that the interaction between organophosphate groups and $Ni\{P_4Mo_6\}_2$ cluster may potentially expedite charge transportation and electron transfer, further enhancing the separation efficiency of photogenerated carriers and augmenting the photocurrent. Overall, the strong light absorption and suitable energy band structure of compound **1** endows its great potential as a PEC sensor for applications.

Levofloxacin (LVF), as a highly effective and versatile fluoroquinolone antibiotic, stands out due to its broad-spectrum antibacterial activity. It plays a crucial role in managing bacterial infections in both humans and animals [20–23]. However, the recent LVF overuse worsens contamination, endangering health [24–26]. Given the crucial importance of food safety, it is crucial to achieve quantitative and sensitive detection of trace LVF. Considering the excellent photo- and electro-chemical property, compound **1** was selected as a PEC sensor toward the LVF detection. The PEC detection performance was evaluated in 0.5 mol/L H_2SO_4 electrolyte under 40 W white light. As shown in Fig. 3a, the current responses of differential pulse voltammetry (DPV) curves significantly increased with the LVF concentrations continuously rising from 0.1 μmol/L to 1.0 μmol/L, which suggested the sensitive and rapid electrochemical response of compound **1** to the variations in LVF concentration. Notably, the response signals of compound **1** exhibited a distinct linear relationship with LVF concentration, with linear regression equation of $I(\mu A) = 264.02 \times C(\mu mol/L) + 11.29$, where C and *I* represent the concentration of LVF and the response current observed from the DPV plots (Fig. 3b). Based on the principle of a signal-to-noise ratio of 3, the detection (LOD) for LVF by compound **1** was calculated to be 4.61 nmol/L (1.67 ppb), and the sensitivity was determined to be 264.02 μA L/μmol. Such performance is superior to most reported noble-metal materials and POM-based sensors (Table S10 in Supporting information).

As comparison, the PEC detection performance of $Ni\{P_4Mo_6\}_2$-based compound **2** was also assessed. As shown in Figs. 3b and c, compound **2** displays *ca.* 78 μA increment on response current with increasing the LVF concentration from 0.1 μmol/L to 1.0 μmol/L, from which the sensitivity and LOD of compound **2** were obtained to be 85.6 μA L/μmol and 6.8 nmol/L (2.46 ppb). It can be found that the detection sensitivity of **1** is 3.08 times higher than that of compound **2**, and its LOD for LVF is 0.68 times lower than that of compound **2** (6.8 nmol/L). The bib component shows no detection activity toward LVF (Fig. S9 in Supporting information). Considering the only difference between the $Ni\{(PhP)_4Mo_6\}_2$ and $Ni\{P_4Mo_6\}_2$ clusters in the two compounds, the improvement in performance should be attributed to the covalent functionalization of phenyl phosphate on the $Ni\{P_4Mo_6\}_2$ cluster.

To further explore the mechanism that the covalent functionalization of phenyl phosphate enhances detection performance,

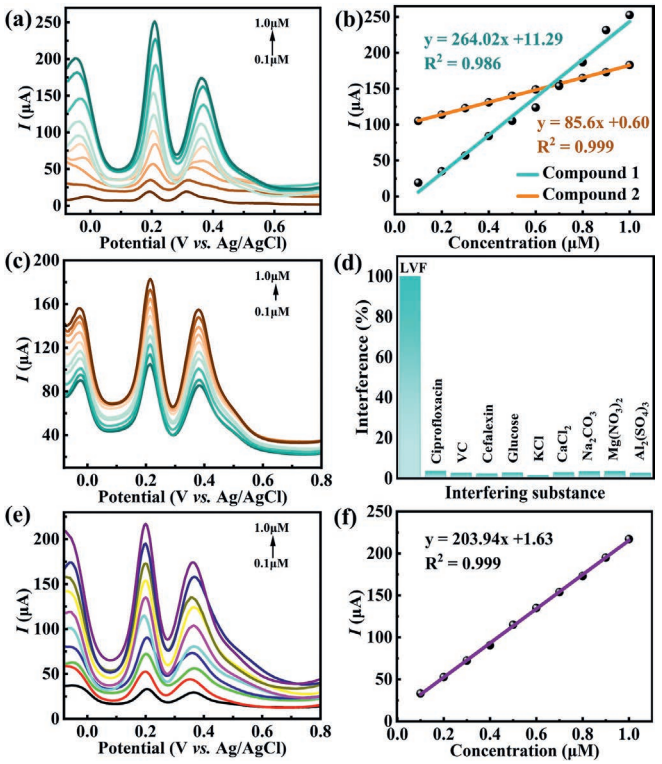


Fig. 3. (a) DPV curves of compound **1** in 0.5 mol/L H_2SO_4 with continuous addition of LVF under visible light illumination. (b) The linear dependence curves of compounds **1-2**. (c) DPV curves of compound **2** in 0.5 mol/L H_2SO_4 with continuous addition of LVF under visible light illumination. (d) Percentage changes in response signal to the addition of different interfering ion (500 μmol/L) in detection system (ciprofloxacin, VC, cefalexin, glucose, K^+, Ca^{2+}, Mg^{2+}, Cl^-, SO_4^{2-} and CO_3^{2-}). (e) DPV curves of compound **1** in acidified milk sample with continuous addition of LVF. (f) The linear dependence curve of compound **1**.

the detection experiments under dark reaction conditions were conducted. As shown in Fig. S10 (Supporting information), under the dark condition, compound **1** shows a LOD of 10.56 nmol/L (3.82 ppb) toward LVF, with a sensitivity of 115.3 μA L/μmol. It can be found that the sensitivity under PEC condition is 2.29 times higher than that in dark condition, and the LOD value is reduced by 0.44 times compared to that in dark condition. These results verified the excellent PEC detection performance of $Ni\{(PhP)_4Mo_6\}_2$-based compound **1**. Moreover, the electrochemical impedance spectroscopy (EIS) measurements in Fig. S11a (Supporting information) showed that under light irradiation compound **1** displayed a smaller charge transfer impedance of 40 Ω compared to compound **2** (50 Ω) and that in dark condition (47 Ω) (Fig. S11b in Supporting information), which suggested the rapid separation and transfer capacities of photogenerated carriers, expediting the electron transfer within the LVF oxidation process and amplifying the response signal.

Additionally, the detection selectivity and anti-interference capability of such PEC sensors were investigated by adding a series of interference agents such as ofloxacin, norfloxacin, ciprofloxacin, VC, cefalexin, glucose, K^+, Ca^{2+}, Mg^{2+}, Cl^-, SO_4^{2-} and CO_3^{2-} to the LVF detection system. As shown in Fig. 3d and Fig. S12 (Supporting information), compound **1** only produces significant response signals to the addition of LVF or ofloxacin due to their almost same structures, while the impact of other interfering substances on the response current does not exceed 5 %. This result reveals the strong anti-interference ability and high selectivity of compound **1** for LVF detection, providing a possibility for LVF detection in practical environments.

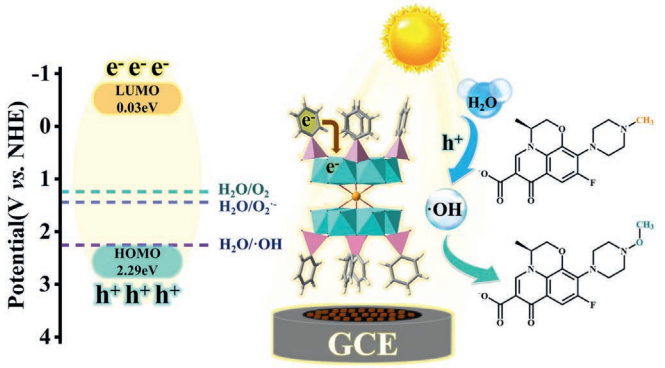


Fig. 4. The proposed mechanism of compound **1** in the PEC detection of LVF.

To further validate its practical applicability, the LVF in milk samples was determined using compound **1** as PEC sensor. Considering the absence of LVF in commercial dairy samples, a specific quantity of LVF was introduced into the actual sample after acidification. As shown in Figs. 3e and f, experiments showed that the sensitivity and LOD of compound **1** for LVF in milk samples were 203.94 μA L/μmol and 5.94 nmol/L (2.15 ppb), respectively. These results are almost consistent with the outcomes in pure water, indicating the good practicality of compound **1**. Furthermore, compound **1** demonstrated excellent structural stability and photoelectrochemical durability, maintaining the stable response current under continuous operation for 24 h at different temperatures of 0, 25, and 50 °C (Figs. S13 and S14 in Supporting information), respectively. Additionally, the possible mechanism of compound **1** for PEC sensing LVF was proposed (Fig. 4). Upon exposure to visible light, Ni{$(PhP)_4Mo_6$}$_2$-based compound **1** was easily excited to generate photoelectrons and holes that could be fast separated in the assistance of an external electric field. The photogenerated holes (h^+) could interact with H_2O to form ·OH radical (Fig. S15 in Supporting information), which could oxidize the tertiary amine at N position of the piperazine ring in LVF to form oxidized LVF (Eqs. S1–S3 in Supporting information) [27,28]. Such photo-assisted electrochemical process facilitates the oxidation of LVF, which produce amplified electrical signals correlated to the concentrations of LVF, thereby enhancing sensing efficiency.

In summary, a kind of Ni{$(PhP)_4Mo_6$}$_2$-based hybrid was constructed as a PEC sensor for detecting trace LVF at the nmol/L level. Owing to the phenylphosphonate covalent functionalization, compound **1** showed narrower band gap, suitable energy band structure and enhanced light absorption, which accelerated the production and utilization of photogenerated electrons/holes, achieving excellent PEC detection performance. The LOD for LVF is as low as 4.61 nmol/L, and corresponding sensitivities for detecting LVF is recorded at 264.02 μA L/μmol, which is superior to most noble-metal materials and POM-based sensors. In addition, compound **1** exhibits high selective and reliable performance in analyzing LVF in environmental samples such as milk. This work offers significant insights for the design of high-efficiency PEC sensors for environmental surveillance.

Declaration of competing interest

The authors declare that they have no known competing financial interests or personal relationships that could have appeared to influence the work reported in this paper.

CRediT authorship contribution statement

Meng-Si Guo: Writing – original draft, Methodology, Investigation, Data curation. **Chun-Xiao Yin:** Formal analysis, Data curation. **Zi-Yi Zhang:** Validation, Formal analysis. **Yuan-Yuan Ma:** Writing – review & editing, Writing – original draft, Supervision, Funding acquisition, Conceptualization. **Jing Du:** Writing – review & editing, Supervision, Funding acquisition, Conceptualization. **Zhan-Gang Han:** Writing – review & editing, Writing – original draft, Validation, Supervision, Funding acquisition, Conceptualization.

Acknowledgments

This work was supported by the National Natural Science Foundation of China (Nos. 22371065, 22471056, 22301058), the Natural Science Foundation of Hebei Province (Nos. B2024205033, B2024205007, B2020205008, B2022205005), the Science and Technology Project of Hebei Education Department (No. QN2023049), the China Postdoctoral Science Foundation funded project (No. 2021TQ0095), the Project of Science and Technology Department of Hebei Province (No. 22567622H), the Science Foundation of Hebei Normal University (No. L2023B51), Chemistry Postdoctoral Research Station at Hebei Normal University.

Supplementary materials

Supplementary material associated with this article can be found, in the online version, at doi:10.1016/j.cclet.2025.111158.

References

[1] S.S. Wang, G.Y. Yang, Chem. Rev. 115 (2015) 4893–4962.
[2] J.M. Cameron, G. Guillemot, T. Galambos, et al., Chem. Soc. Rev. 51 (2022) 293–328.
[3] T. Ma, R. Yan, X.Z. Wu, et al., Adv. Mater. 36 (2024) 2310283.
[4] H.X. Bi, M.S. Guo, J. Du, Y.Y. Ma, Z.G. Han, Coord. Chem. Rev. 518 (2024) 216092.
[5] H. Song, M.S. Guo, J.F. Wang, et al., Polyoxometalates 3 (2024) 9140065.
[6] H.X. Bi, X.Y. Yin, J.Y. He, et al., Rare Met. 42 (2023) 3638–3650.
[7] W.T. An, X.J. Zhang, J.Q. Niu, Y.Y. Ma, Z.G. Han, Chin. Chem. Lett. 33 (2022) 4400–4404.
[8] Y.L. Wang, Y.Y. Ma, Q. Zhao, L. Hou, Z.G. Han, Sens. Actuator. B 305 (2020) 127469.
[9] K. Wieszczycka, K. Staszak, M.J. Woźniak-Budych, et al., Coord. Chem. Rev. 436 (2021) 213846.
[10] M.A. Neouze, U. Schubert, Monatsh. Chem. 139 (2008) 183–195.
[11] L. Zhang, J.M. Cole, Mater. Interfaces 7 (2015) 3427–3455.
[12] S.J. Li, Y.F. Zhou, N.N. Ma, et al., Angew. Chem. Int. Ed. 59 (2020) 8537–8540.
[13] G. Cao, R.C. Haushalter, K.G. Strohmaier, Inorg. Chem. 32 (1993) 127–128.
[14] M.I. Khan, Q. Chen, J. Zubieta, Inorg. Chim. Acta 235 (1995) 135–145.
[15] A. Gammersbach, P. Angenault, W.F. Holderich, W. Clegg, M.R.J. Elsegood, Polyhedron 17 (1998) 2535–2541.
[16] L.Y. Duan, F.C. Liu, X.L. Wang, et al., J. Mol. Struct. 705 (2004) 15–20.
[17] D. Gouveia, B. Yilmaz, P. Cevik, W.M. Johnston, Dent. Mater. 38 (2022) 1452–1458.
[18] L.P. Yang, G.H. Dong, D.L. Jacobs, et al., Catalysis 352 (2017) 274–281.
[19] S. Cong, J.H. Yu, B.J. Liu, W. Teng, Y.B. Tang, New J. Chem. 46 (2022) 15227–15243.
[20] N. Asseray, C. Bourigault, D. Boutoille, et al., Int. J. Antimicrob. Agents 47 (2016) 478–481.
[21] L. Fu, S.D. Mao, F. Chen, et al., Chemosphere 297 (2022) 134127.
[22] F.A. Ansari, S. Manuel, R. Dwivedi, et al., Indian J. Nephrol. 29 (2019) 424–426.
[23] Y.T. Zhang, X.M. Qi, X.F. Zhang, et al., Carbohyd. Polym. 340 (2024) 122306.
[24] N.A. Dafale, U.P. Semwal, P.K. Agarwal, P. Sharma, G.N. Singh, J. Pharm. Anal. 5 (2015) 18–26.
[25] A.A. Salem, H.A. Talanta 88 (2012) 104–114.
[26] Z.Y. Zhu, X. Bai, Y.T. Ji, Sens. Actuator. B Chem. 377 (2023) 133076.
[27] K. Bhimaraya, J. Manjunatha, K. Moulya, et al., Chemosensors 11 (2023) 191.
[28] M.H. Ghanbari, A. Khoshroo, H. Sobati, et al., Microchem. J. 147 (2019) 198–206.